

# The Effect of SERCA2 Transfected Stem Cells on Induced Wound in Type1 Diabetes of Male Albino Rat Model Compared to Stem Cells

*Maha Baligh Zickri<sup>1,2</sup>, Hala Ahmed El Sherif<sup>1</sup>, Zainab Mohammad Altaib<sup>3</sup>, Ahlam mohamed Gharieb<sup>3</sup>, Amal Moloud Alshebani<sup>4</sup>, Radia Mosbah Ahmed<sup>4</sup> and Amany Elsayed Hamoud<sup>5</sup>*

## Original Article

<sup>1</sup>Department of Medical Histology, Faculty of Medicine, Cairo University, Egypt

<sup>2</sup>Faculty of Oral and Dental Medicine, Future University, Egypt (FUE)

<sup>3</sup>Department of Medical Histology, Faculty of Medicine, Helwan University, Egypt

<sup>4</sup>Department of Biology, Faculty of Medicine, AlZawia University, Lybia

<sup>5</sup>Department of Anatomy and Embryology, Faculty of Medicine, Cairo University, Egypt

## ABSTRACT

**Background and Objectives:** Diabetic wounds are difficult to manage. For cell proliferation, migration, differentiation and regeneration, intracellular Ca<sup>2+</sup> equilibrium is crucial. Sarcoplasmic reticulum Ca<sup>2+</sup> ATPase2 (SERCA2) has been shown to control Ca<sup>2+</sup> level in keratinocytes. Adipose derived mesenchymal stem cells (AdMSCs) are essential for the repair of wounds. The therapeutic effect of SERCA2 gene modified AdMSCs was studied and compared to that of AdMSCs on experimentally induced diabetic wound type 1.

**Methods and Results:** 42 male rats were classified into: Donation group: three were used for stem cell culture, phenotyping, tagging and SERCA2 preparation. 1<sup>st</sup> Group I (Control Group): nine rats, 2<sup>nd</sup> Group (Wounded Group): ten rats were injected with streptozotocin (STZ) intraperitoneal (IP) 50 mg, then rats were exposed to wound induction (1x1cm skin incision). 3<sup>rd</sup> Group (AdMSCs Therapy): ten rats, injected IP with 1x10<sup>6</sup> AdMSCs. 4<sup>th</sup> Group (SERCA2 modified AdMSCs Group): ten rats, injected IP with 1x10<sup>6</sup> SERCA2 modified AdMSCs. By end of 1<sup>st</sup> and 3<sup>rd</sup> weeks, induced diabetic wound surface area was measured. 1<sup>st</sup> 2<sup>nd</sup> 3<sup>rd</sup> and 4<sup>th</sup> Groups were scarified three weeks after diagnosis of diabetes. Serological, biochemical, phenotypic and quantitative studies were done. In 2<sup>nd</sup> group, inflammatory, fibrotic and degenerative changes were seen in the wound area and in intact skin. In 3<sup>rd</sup> and 4<sup>th</sup> groups these changes were ameliorated, more noticed in 4<sup>th</sup> group. In the 2<sup>nd</sup> group, a significant difference was found in wound surface area. Phenotypic and quantitative changes were confirmed by serum glucose, skin Ca<sup>2+</sup> concentration and western blot analysis.

**Conclusions:** SERCA2 gene modified AdMSCs therapy exerted a more pronounced ameliorating effect versus AdMSCs' effect.

**Received:** 21 October 2022, **Accepted:** 05 November 2022

**Key Words:** Diabetes mellitus, immunohistochemistry, SCs, SERCA2, wound.

**Corresponding Author:** Amany Hamoud, MD, Department of Medical Histology, Faculty of Medicine, Kasr-Elainy Hospital, Cairo University, Egypt, **Tel.:** +20 10 2036 4428, **E-mail:** dramanyhamoud@gmail.com

**ISSN:** 1110-0559, Vol. 47, No. 1

## INTRODUCTION

Diabetes wounds are chronic in nature because they regularly reoccur and heal slowly, which not only raises the cost of medical care but also significantly lowers the quality of life for diabetic patients. Clinics' current go-to treatments, as debridement, dressings and infection management, haven't produced satisfying outcomes. Therefore, it is essential to find more efficient therapeutic methods that can accelerate the healing of diabetic wounds<sup>[1]</sup>. One of the main effects of diabetes is impaired wound healing, which is characterised by persistent oxidative stress, delayed re-epithelialization and protracted inflammation<sup>[2]</sup>.

Administration of stem cells of mesenchymal origin is a new treatment for chronic wound healing and repair

that has gained popularity in recent years. MSCs reside in normal skin and enhance regenerative reconstruction of injured skin in diabetics<sup>[3]</sup>. Adipose-derived stromal vascular fraction, which contains MSCs, may improve healing and preserve function<sup>[4]</sup>.

Skin barrier formation in cultured keratinocytes was established by restoration of the calcium level and was knocked down after treatment of cells by high glucose simulating hyperglycemia state<sup>[5]</sup>. Calcium ion (Ca<sup>2+</sup>) homeostasis influences skin barrier formation and is important for division, differentiation and development of keratinocytes junctions<sup>[6]</sup>. Sarcoplasmic reticulum Ca<sup>2+</sup>-ATPase2 (SERCA2) was proved to be a key protein involved in restoration of Ca<sup>2+</sup> in endoplasmic reticulum

(ER) in keratinocytes. SERCA2 role in proliferation, cell-to-cell adhesion and microbial barrier integrity has been documented<sup>[7]</sup>.

Introduction of a gene into stem cells (Transfection) in tissue cultures was authorized. Lipofectamine maintained its popularity, being simple to use, inexpensive and adaptable to throughput mechanisms<sup>[8]</sup>.

The current work attempted to evaluate the therapeutic effect of SERCA2 gene modified AdMSCs and compare it to that of AdMSCs on experimentally induced wound in type 1 diabetes mellitus (T1DM).

## MATERIALS AND METHODS

### *Experimental Animal Design*

The present work was carried on 42 male albino rats, their age was 3 months and their body weight ranged 180-200 grams. They were divided into the following groups and housed in accordance with Cairo University's guidelines of Institutional Animal Care and Use Committee (CU-IACUC).

### *Donation Group*

Three rats, 2 of which were used for isolation, culture, phenotyping and tagging. In addition, a part of skin of the 3<sup>rd</sup> rat was homogenized and processed for SERCA2 preparation.

**1<sup>st</sup> Group (Control Group):** It constituted 9 rats that represented the experimental 2<sup>nd</sup>, 3<sup>rd</sup> and 4<sup>th</sup> groups. One IP injection of 0.5 ml citrate buffer (CB) was given to 1<sup>st</sup> 3 rats corresponding to wounded group. 2<sup>nd</sup> 3 rats were injected IP with 1ml of phosphate buffered saline (PBS). 4 days after the diagnosis of diabetes, in addition to CB. 3<sup>rd</sup> 3 rats were injected IP with 1.5 µl of lipofectamine along with citrate buffer and PBS.

**2<sup>nd</sup> Group (Diabetic wounded):** It constituted 10 rats. Induction of diabetes was exerted by IP injection of STZ once (Sigma Company, St. Louis, Mo, USA) as 1 g vial powder in a dose of 50 mg/kg<sup>[9]</sup>. Each dose was dissolved in 0.5 ml citrate buffer after being weighed using a digital scale. Diabetes was identified three days after the STZ injection by checking the blood glucose Three days following STZ injection, diabetes was confirmed by measuring the blood glucose level. The animals were considered diabetic if the blood glucose level was greater than 200 mg/dl, diabetes was diagnosed<sup>[10]</sup>.

The rats were exposed to wound induction on the 4<sup>th</sup> day. Wound induction was performed by anaesthetizing the rats, Ketalar, (Barcelona, Spain) was injected intramuscular in a dose of 35 mg/kg. Using sterile techniques the hair was shaved on the middle part of back of rat, where a skin incision of 1x1cm was made using a sterile scalpel and 1cm<sup>2</sup> of skin was removed<sup>[11]</sup>. Every day, the injured site was rinsed with regular saline after applying betadine to the wound.

**3<sup>rd</sup> Group (Diabetic wounded and Non-transfected AdMSCs treated):** It constituted ten rats. 1x10<sup>6</sup> cultivated and PKH26 tagged rat AdMSCs suspended in a tube containing 1ml PBS were injected IP the day after diabetes diagnosis<sup>[12]</sup>.

**4<sup>th</sup> Group (Diabetic wounded and SERCA2 gene modified AdMSCs treated):** It constituted 10 rats. On the 4<sup>th</sup> day, 1x10<sup>6</sup> of cultivated and green fluorescent protein (GFP) tagged SERCA2 gene modified AdMSCs were injected IP.

Sacrifice was performed in control and corresponding experimental groups, 3 weeks after diagnosis of diabetes.

### *Source and culture of non-transfected rat AdMSCs<sup>[13]</sup>*

Rats were cut open at the abdomen, their adipose tissues were removed, and they were then put to death with carbon dioxide (CO<sub>2</sub>) in sterile settings. All of the adipose tissues were collected and incubated in Dulbecco's modified Eagle's medium (DMEM), (GIBCO/BRL) with 10% foetal bovine serum (FBS), after being cleaned with saline solution. Ficoll/Paque (Pharmacia) was used to separate nucleated cells using a density gradient, and the cells were then resuspended in full culture media with 1% penicillin-streptomycin (GIBCO/BRL). As a primary culture or after the formation of large colonies, cells were incubated for 12–14 days at 37° C in 5% humidified CO<sub>2</sub>. After two PBS washes, cultures were trypsinized with 0.25% trypsin in 1 millimolar EDTA (GIBCO/BRL) for five minutes at 37° C once substantial colonies (80–90% confluence) had formed. Cells were resuspended in serum-supplemented media following centrifugation (at 2400 rpm for 20 minutes). Incubation in a 50 cm<sup>2</sup> Falcon culture flask are considered 3<sup>rd</sup>-passage cultures. The adhering cell colonies were trypsinized and counted on day 14.

### *Immunohistochemical markers of nontransfected AdMSCs<sup>[14]</sup> and flow cytometry<sup>[15]</sup>*

Using hemocytometer, 1x10<sup>6</sup> cells/ml were incubated with 10µl of monoclonal antibodies: CD34 and CD44 (Beckman coulter, USA) for 20 minutes. Then 2% fraction crystallizable solution (FCS) in 2 ml PBS were placed. High speed centrifugation for 5 minutes was done and supernatant was discarded. CYTOMICS Flow Cytometer 500 (Beckman coulter, USA) cell analysis was performed using CXP Software version 2.2.

### *PKH26 tagging of nontransfected AdMSCs<sup>[16]</sup>*

4<sup>th</sup> passage collected non-transfected AdMSCs cells were tagged with PKH26 fluorescent linker dye to be able to be examined by fluorescent microscopy.

### *SERCA2 gene extraction<sup>[17]</sup>*

Using a Polytron homogenizer skin specimens were homogenized. SERCA2 primer was processed in homogenates for ribonucleic acid (RNA) extraction. Then complementary DNA (cDNA) was synthesized by reverse transcription.

**Lipid mediated gene transfection and GFP tagging of gene modified AdMSCs**

Incubation in serum-free DMEM of 1.5 µL Lipofectamine 3000 reagent<sup>[18]</sup> and 1.5 µg SERCA2 gene tagged with GFP<sup>[19]</sup> was done. GFP fuses to specific loci on SERCA2. 4 hours later culture media were. To assess transfection efficiency, morphology and viability cells tagged with GFP were examined by fluorescence microscopy. Cells were incubated in 250 µL of mixture of Tryp reagent at 37°C for 10 minutes. then analyzed by flow cytometry.

**Wound surface area measurements**

Wound boundary was used to estimate the wound surface area. Tissue differentiation depends on different color of unhealthy tissue (Figures 1a,1c). A number of measurement techniques using images are referred

to as photogrammetry. Digital photoplanimetry is the measurement of planes using digital images. These markers are positioned close to the wound and are visualized in the photo with the wound. A true scale of the image should be guaranteed, With the Sony digital camera's 12 Mega Pixels, photos of wounds were taken at a distance of 15 cm from wound. The image was afterwards processed using the image J software to determine the exact measurements (Figure 1b). The polygon selection in the tools bar was used to localize the wound and image J measured it. A second image of 1 cm<sup>2</sup> square was obtained as a standard for calibrating wound measurements in cm<sup>2</sup>, and it had a resolution of 102704 pixels. By the ends of first and third weeks, photographs of wounds were taken.  $A/k^2$  is the formula for calculating the surface area in units of area S, where A is number of pixels and k is number of pixels per unit of distance (calibration coefficient)<sup>[20]</sup>.

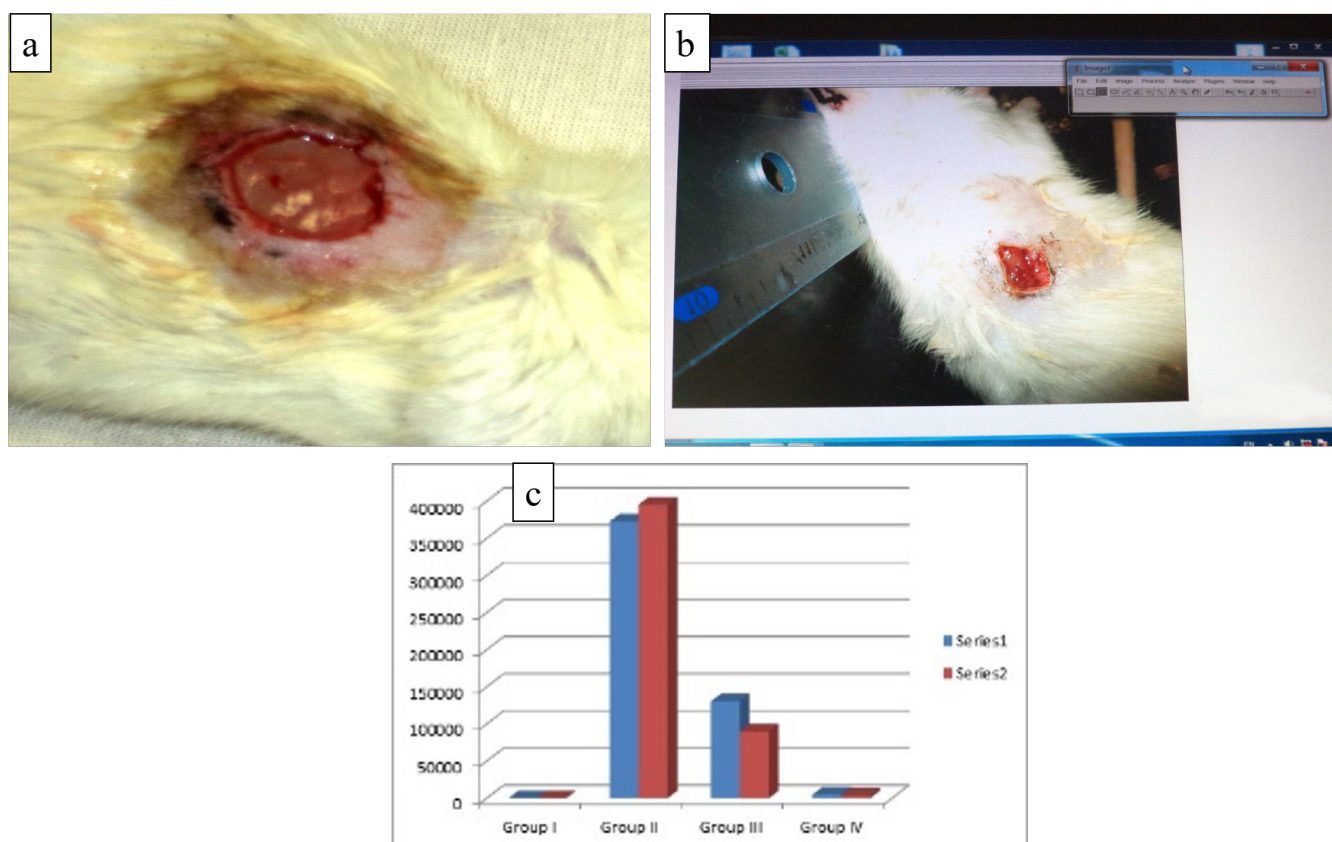


Fig. 1 showing (a) Wound induction (b)Tracing and measuring the wound size with image J. (c) Histogram of wound surface area measurements, series1 (post 1 week), series 2 (post 3 weeks) of treatment.

**Serum glucose level**

At the end of the experiment, blood samples were obtained from tail veins from control and experimental groups for serum glucose values determination.

The rats were euthanized by cervical dislocation<sup>[21]</sup>. Half the wound and 1cm of surrounding skin samples were homogenized to perform:

Skin Ca<sup>2+</sup> concentration: Using a homogenizer, 1 gm of skin was homogenised in 10 ml of ordinary saline (Ortoalresa, Spain). For 15 minutes, centrifugation at 1000

x g was exerted. In epindorff tubes, the supernatant was gathered and kept in deep freezer. Ca<sup>2+</sup> concentration was determined using colorimetric method. Quimica Clinica Aplicada SA (Amposta, Spain) provided the analytical kits<sup>[22]</sup>.

Western blot analysis: SERCA2 protein content was estimated and normalized to actin<sup>[23]</sup>.

**Phenotypic Study**

2<sup>nd</sup> half of samples including the wound and 1cm of surrounding skin were fixed for 48 hours using 10% formol



saline. 5µm thick sections were used for:

1. Hematoxylin and Eosin (H&E) staining<sup>[24]</sup>
2. Masson's trichrome staining<sup>[25]</sup>.
3. Immunohistochemical staining<sup>[26]</sup> for:
  - a. Cytokeratin (CK) 3 (MS-1447-R7, Lab Vision Corporation, USA) immunostaining, for demonstration of cytoskeletal protein.
  - b. Caspase3 (RB-1197-R7, Lab Vision Corporation, USA) immunostaining, the marker for apoptosis.
  - c. Proliferating cell nuclear antigen (PCNA) (Clone PC10, Lab Vision Corporation, USA) immunostaining

Prediluted 1ry mouse monoclonal CK3 antibody was added 0.1 ml for 60 minutes. The reaction is cytoplasmic. Sections of human cornea serve as +ve control. Prediluted 1ry rabbit polyclonal caspase3 antibody was added 0.1 ml for 60 minutes. The reaction is cytoplasmic. Human tonsils serve as positive control. Prediluted 1ry mouse monoclonal PCNA antibody was added 0.1 ml for 60 minutes. The reaction is nuclear. Human skin serve as +ve control. By omitting 1ry antibody addition for negative control preparation.

### **Quantitative Phenotypic Study**

By using computer assisted Leica Qwin 500 LTD (Cambridge, UK) image analyzer, the following was assessed:

1. Distance between epidermal edges of wound using interactive measurements menu in 10 non overlapping fields using x100 magnification.
2. Area% of pale collagen fibers
3. Area% of CK3 immunoexpression (IE).
4. Area% of caspase3 IE using binary mode in 10 non overlapping fields using x200 magnification.
5. Count of PCNA +ve nuclei (N) using interactive measurements menu.

### **Quantitative polymerase chain reaction (qPCR)**

Skin samples that were formalin-fixed and paraffin-embedded (FFPE) were used<sup>[27]</sup>. The SERCA2 primer (5'-oligonucleotide primer 5'-AAGTGCAATACCTCACTCG-3' and 3'-oligonucleotide primer 5'-GATCAGCAGCAGACATATC-3') was used for reverse transcription. After preparing the master mixture, adding it to RNA/primer combination, and leaving it at room temperature for two minutes. After adding 1µl RNAase it was incubated at 37°C for 20 min. Prior to usage, first strand cDNA was kept at -20°C. Gene-specific and reverse primer pairs were combined, and primer concentrations were standardised. The ABI Prism standard

deviation score (SDS) 7000 was used to build up the PCR program. The software SDS 7000 was used to analyse the results.

### **Statistical Analysis<sup>[28]</sup>**

A Bonferroni post-hoc test was employed to determine which pairs of groups were responsible for any significant ANOVA results. Statistics were considered significant for *P-values* less than 0.05. Version 16 of the Statistical Package for the Social Sciences (SPSS) was used to perform the calculations.

## **RESULTS**

Reduced activity and increased urine output were recorded in the diabetic group. These observations improved by AdMSCs and gene modified AdMSCs therapy. Two rats died few days following STZ injection and were compensated.

### **Immunohistochemical and flow cytometry results of AdMSCs and gene modified AdMSCs**

Spindle AdMSCs showed +ve membranous CD44 IE and -ve for CD34. 97.2 % of the cells +ve (Figures 1a,b,c). Fluorescent spindle gene modified cells were GFP tagged and represented 95.1 of cells GFP (Figures 1d,e).

### **Wound surface area measurements**

The treated groups revealed significant decrease in surface area versus the diabetic group and in gene modified AdMSCs versus nontransfected AdMSCs treated group ( $P \leq 0.05$ ) (Table1, Figure 1c).

### **Serum glucose level**

The values denoted significant ( $P \leq 0.05$ ) increase in the 2<sup>nd</sup> group versus control and treated groups (Figure 2a).

### **Skin Calcium Ion Concentration level**

The values recorded significant decrease in the 2<sup>nd</sup> group versus other groups and in 3<sup>rd</sup> group versus 1<sup>st</sup> and 4<sup>th</sup> groups (Figure 2b).

### **Western Blot analysis**

The mean SERCA2 protein reported significant decrease in the 2<sup>nd</sup> group versus other groups and in 3<sup>rd</sup> group versus 1<sup>st</sup> and 4<sup>th</sup> groups (Figures 2c,d).

### **Histological phenotyping**

All control rats' sections demonstrated epidermis, dermis, hair follicles, sebaceous glands and hypodermis (Figure 3a). Closer observation showed pale nuclei and basophilic cytoplasm of the basal and spiny layers, dark basophilic granules of the granular layer and flattened non-nucleated keratinized squamous in the horny layer (Figure 3b). Sections of group II recruited wide separation of the wound edges, detached parts of the epidermis, disrupted dermal fibers and detached sebaceous glands. Follicles lined by one layer of cells and multiple micro-follicles were evident (Figure 3c). Closer observation

revealed thin wound edge at one side exhibiting vacuoles and loss of the granules in the granular cell layer (Figure 3d). Sections of group III showed less widely separated edges of the wound, micro follicles, follicles lined by multiple layers of cells and sebaceous glands (Figure 3e). Closer observation showed focal loss of granules in the granular cell layer and few vacuolated keratinocytes (Figure 3f). Sections of group IV demonstrated minimal separation of wound edges, normal appearance of epidermis, multiple micro follicles, multiple sebaceous glands and fully developed hair follicles (Figure 3g). Closer observation showed normal appearance of granular cell layer and reduced thickness of the wound edge (Figure 3h).

First group recruited normal dermal collagen fibers, multiple dermal atypical and multiple pale fibers were observed in 2<sup>nd</sup> group. While, 3<sup>rd</sup> group revealed multiple pale dermal fibers, 4<sup>th</sup> group demonstrated few pale fibers (Figures 4 a,b,c,d).

In cytokeratin3 (CK3) immunostained sections, 1<sup>st</sup> group showed dense +ve IE in some and less dense IE in other epidermal areas and in the lining of follicles (Figure 5a). While in 2<sup>nd</sup> group, dense +ve IE was found in localized areas and less dense IE was observed in other areas of thin epidermis and in hair follicles with reduced lining at the wound (Figure 5b). Loss of CK3 IE was demonstrated in multiple areas of the epidermis and dense +ve IE was seen at the horny layer in some other areas of the intact skin (Figure 5c). On the other hand, 3<sup>rd</sup> group showed dense +ve IE at the horny layer, less dense IE in some areas of the epidermis IE and in the lining of the follicles. Loss of IE was noticed in other areas at the wound (Figure 5d). In addition, less dense +ve IE was detected in multiple areas besides loss of IE in localized epidermal areas and in few follicles (Figure 5e). In 4<sup>th</sup> group, dense +ve IE was demonstrated in some areas, less dense IE in multiple areas of the epidermis and in hair follicles at the wound. In addition localized loss of IE was noticed (Figure 5f). In epidermis and follicles, focal loss of IE was

accidentally found, dense +ve IE in some areas and less dense IE in the rest (Figure 5g).

First group showed +ve caspase 3 IE in few surface keratinocytes (Figure 6a). While, in 2<sup>nd</sup> group +ve IE was found in many keratinocytes and dermal cells (Figure 6b). On the other hand, group III revealed +ve IE in some keratinocytes and dermal cells (Figure 6c). In group IV, +ve IE was evident in few keratinocytes and dermal cells (Figure 6d). First group showed some PCNA +ve nuclei in epidermis, few follicles and sebaceous glands (Figure 6e). While, 2<sup>nd</sup> group revealed few +ve nuclei in epidermis (Figure 6f). On the other hand, 3<sup>rd</sup> group recruited multiple +ve nuclei in epidermis (Figure 6g). In 4<sup>th</sup> group IV, many +ve nuclei were evident in epidermis and in few follicles (Figure 6h).

Multiple PKH26 fluorescent tagged cells were seen in the 3<sup>rd</sup> group and in 4<sup>th</sup> group multiple GFP fluorescent tagged cells were visualized (Figures 7a,b).

### **Quantitative Phenotypic results (Table 2)**

4<sup>th</sup> group compared to 2<sup>nd</sup> and 3<sup>rd</sup>, as well as 3<sup>rd</sup> group compared to 2<sup>nd</sup> group, a significant decrease ( $P \leq 0.05$ ) was reported for mean distance between epidermal margins and mean area% of pale stained collagen fibers. Compared to all groups and to 1<sup>st</sup> and 4<sup>th</sup> groups, mean area% of CK3 showed a significant decline ( $P \leq 0.05$ ) in 2<sup>nd</sup> and 3<sup>rd</sup> groups respectively. On other hand, 2<sup>nd</sup> group showed a significant increase ( $P \leq 0.05$ ) in mean area% of caspase3 compared to other groups, as well as 3<sup>rd</sup> group compared to 1<sup>st</sup> and 4<sup>th</sup> groups. In comparison to all groups, 4<sup>th</sup> group showed an increase ( $P \leq 0.05$ ) in mean area% of PCNA +ve nuclei. Additionally, 3<sup>rd</sup> group showed increase ( $P \leq 0.05$ ) versus 1<sup>st</sup> and 2<sup>nd</sup> groups. Additionally, 1<sup>st</sup> group exhibited increase ( $P \leq 0.05$ ) versus 2<sup>nd</sup> group.

### **PCR results (Table 2)**

A significant ( $P \leq 0.05$ ) decrease in mean SERCA2 gene values was found in 2<sup>nd</sup> group versus all other groups and in 3<sup>rd</sup> group versus 1<sup>st</sup> and 4<sup>th</sup> groups.

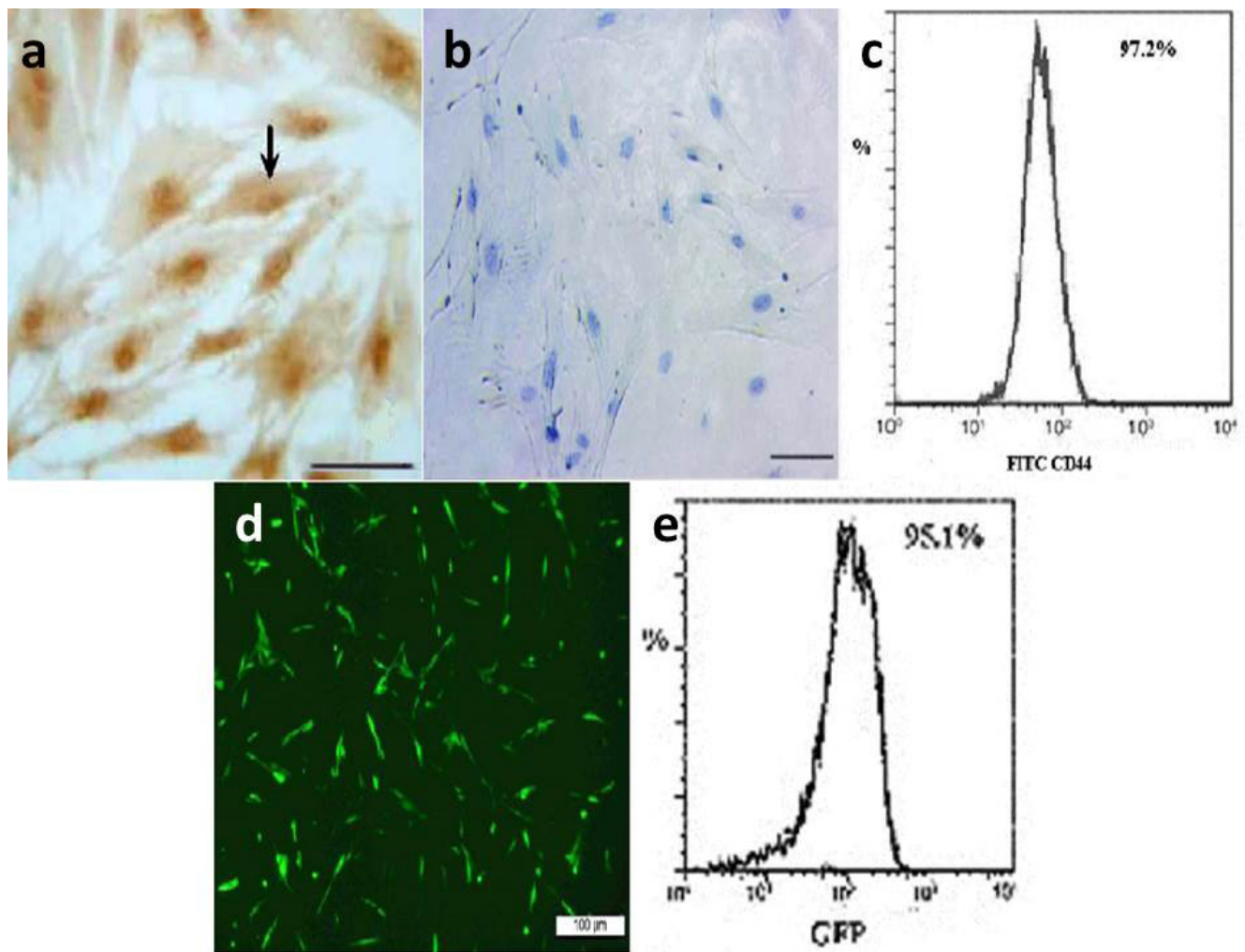


**Fig. 1** showing: (a) CD44 +ve spindle cells (arrow). (b) CD34 -ve immunoreactivity (Phase contrast microscopy x 100). (c) Immunophenotyping of non-transfected AdMSCs 97.2 % are +ve for CD44 (Flow Cytometry). (d) Gene modified cells appearing mostly as spindle fluorescent tagged cells (GFP x 100) (e) Immunophenotyping of gene modified AdMSCs showed 95.1 % of the cells GFP tagged (Flow Cytometry).

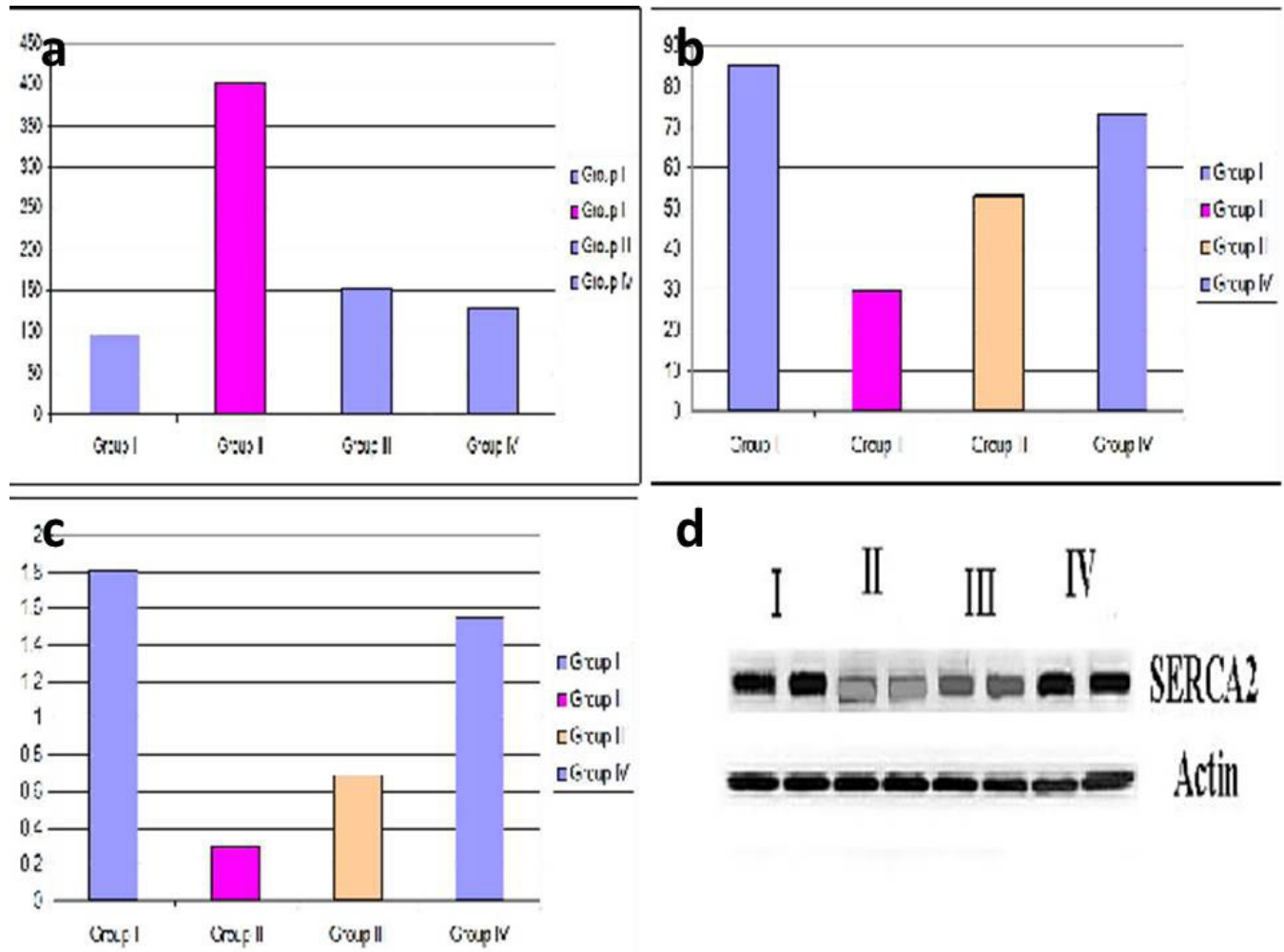
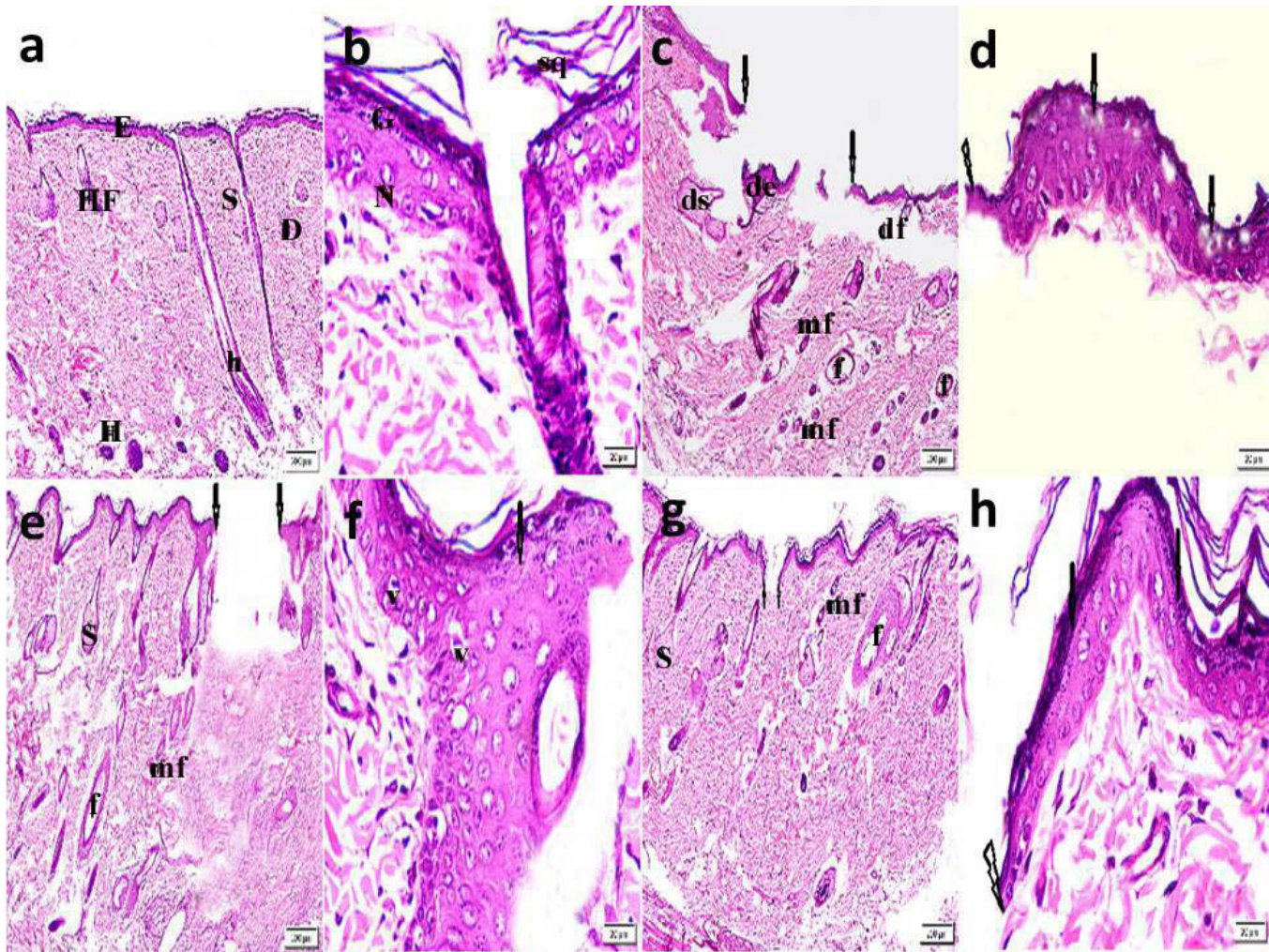


Fig. 2 showing: (a) Mean values of serum glucose level. (b) Mean Ca ion concentration values. (c) Mean Western blot values of SERCA2 protein. (d) Western blot showing SERCA2 protein detected and analyzed (normalized to actin).





**Fig. 3:** skin sections showing (H&E x) (a) in 1st group epidermis (E), dermis (D), a hair follicle (HF), a sebaceous gland (S) and hypodermis (H) (x 40). (b) pale nuclei (N) and basophilic cytoplasm of basal and spiny layers, dark basophilic granules (G) of granular and keratinized squamous (sq) in horny layer (x 400). (c) in 2nd group wide separation of wound edges (arrows), detached parts of epidermis (de), disrupted fibers (df) and detached sebaceous gland (ds). Note follicles (f) lined by one layer of cells and microfollicles (mf) (x 40). (d) thinned wound edge (serrated arrow), vacuoles and loss of granules (arrows) in granular layer (x 400). (e) in 3rd group less widely separated edges of wound (arrows), micro follicles (mf), follicles (f) lined by multiple layers of cells and sebaceous glands (S) ( x 40). (f) focal loss of granules (arrow) in granular layer and few vacuolated (v) keratinocytes (x 400). (g) in 4th group exhibiting minimal separation of wound edges (arrows), normal appearance of epidermis, multiple micro follicles (mf), multiple sebaceous glands (S) and fully developed hair follicles (f) (x 40). (h) normal appearance of granular layer (arrows) and reduced thickness of wound edge (serrated arrow) ( x 400).



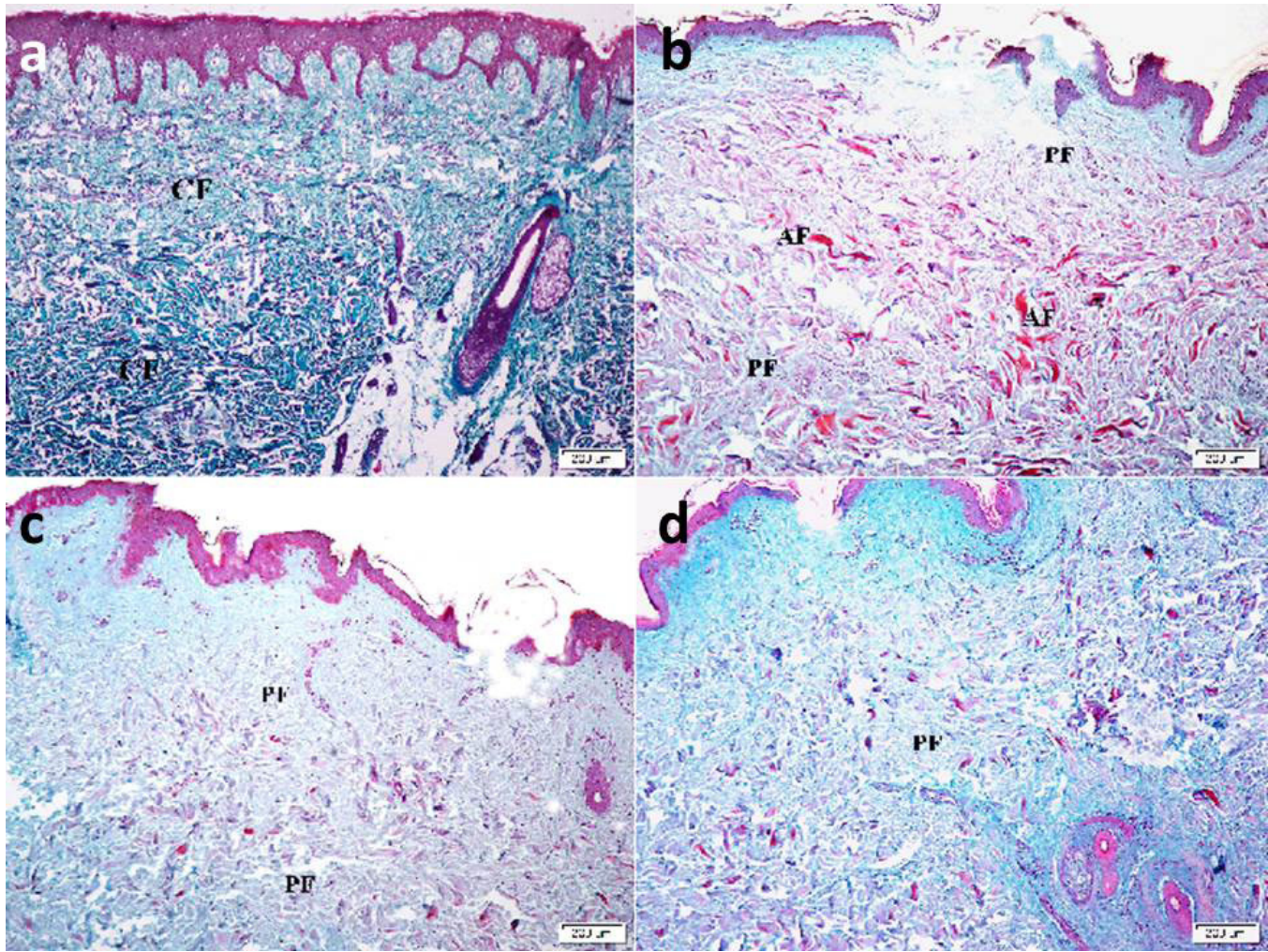


**Fig. 4** showing: (a) normal collagen fibers (CF) in dermis of 1st group. (b) multiple atypical fibers (AF) and multiple pale fibers (PF) in dermis of 2nd group. (c) multiple pale fibers (PF) in dermis of 3rd group. (d) few pale fibers (PF) in dermis of 4th group (Masson's Trichrome, x 40).



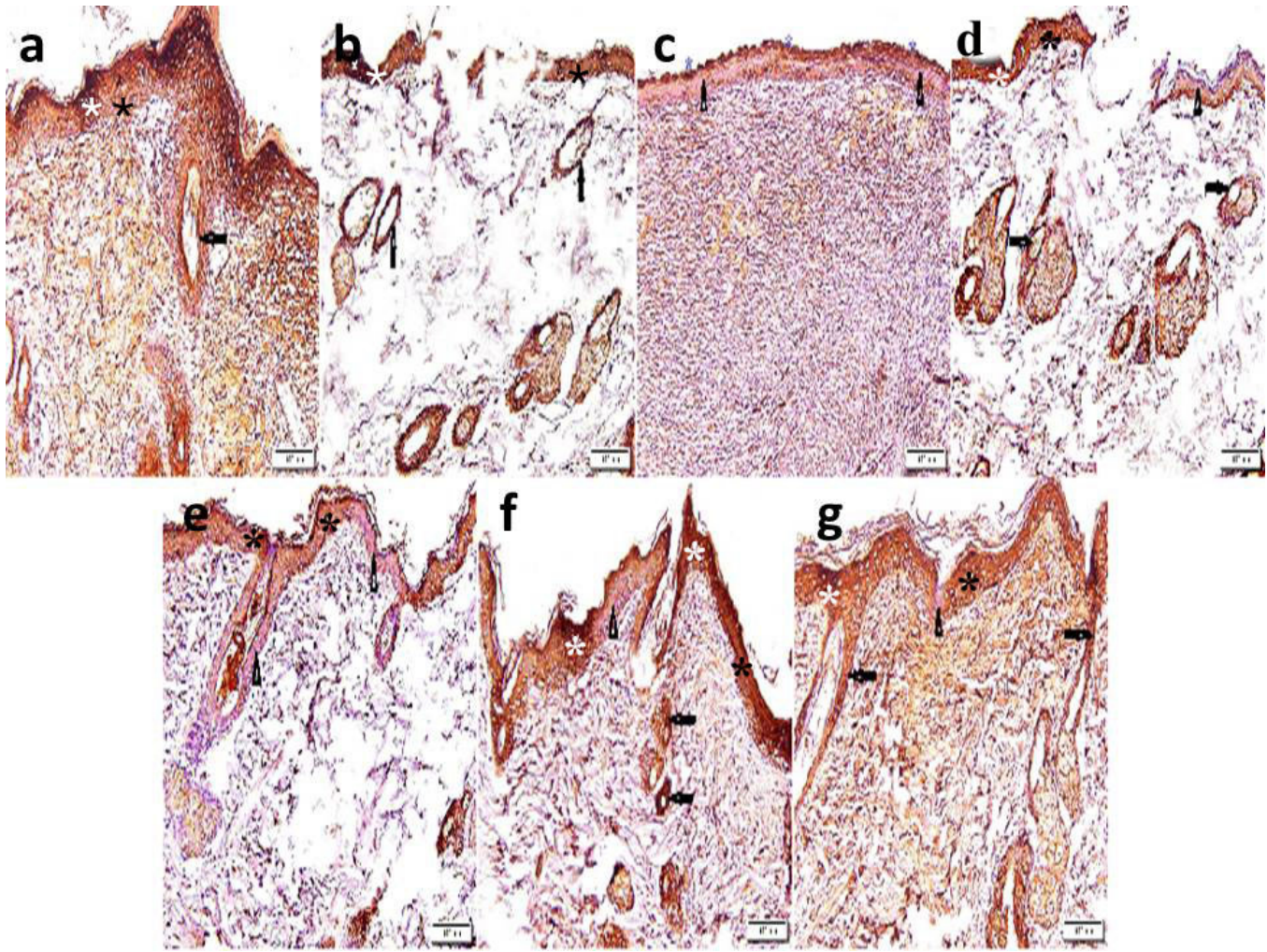


**Fig. 5** showing: (a) dense +ve IE (white star) in some areas and less dense IE (black star) in other areas of epidermis and in hair follicles (arrow) of 1st group. (b) dense +ve IE (white star) in localized areas and less dense IE (black star) in other areas of thin epidermis and in hair follicles with reduced lining (arrows) at wound in 2nd group. (c) loss of IE (triangle) in multiple areas of epidermis and dense +ve IE (blue star) at horny layer in 2nd group. (d) dense +ve IE (blue star) at horny layer, less dense IE (black star) in other areas of epidermis and in follicles (arrows) at wound. Note loss of IE (triangle) in some areas in 3rd group. (e) less dense +ve IE (black star) in multiple areas and loss of IE (triangle) in localized areas of epidermis, in addition to a follicle in 3rd group. (f) dense +ve IE (white star) in some areas and less dense IE (black star) in multiple areas of epidermis and in hair follicles (arrows) at wound. Note localized loss of IE (triangle) in 4th group. (g) focal loss of IE (triangle), dense +ve IE (white star) in some areas and less dense IE (black star) in rest of epidermis and in hair follicles (arrows) in 4th group (CK3 immunostaining, x100).



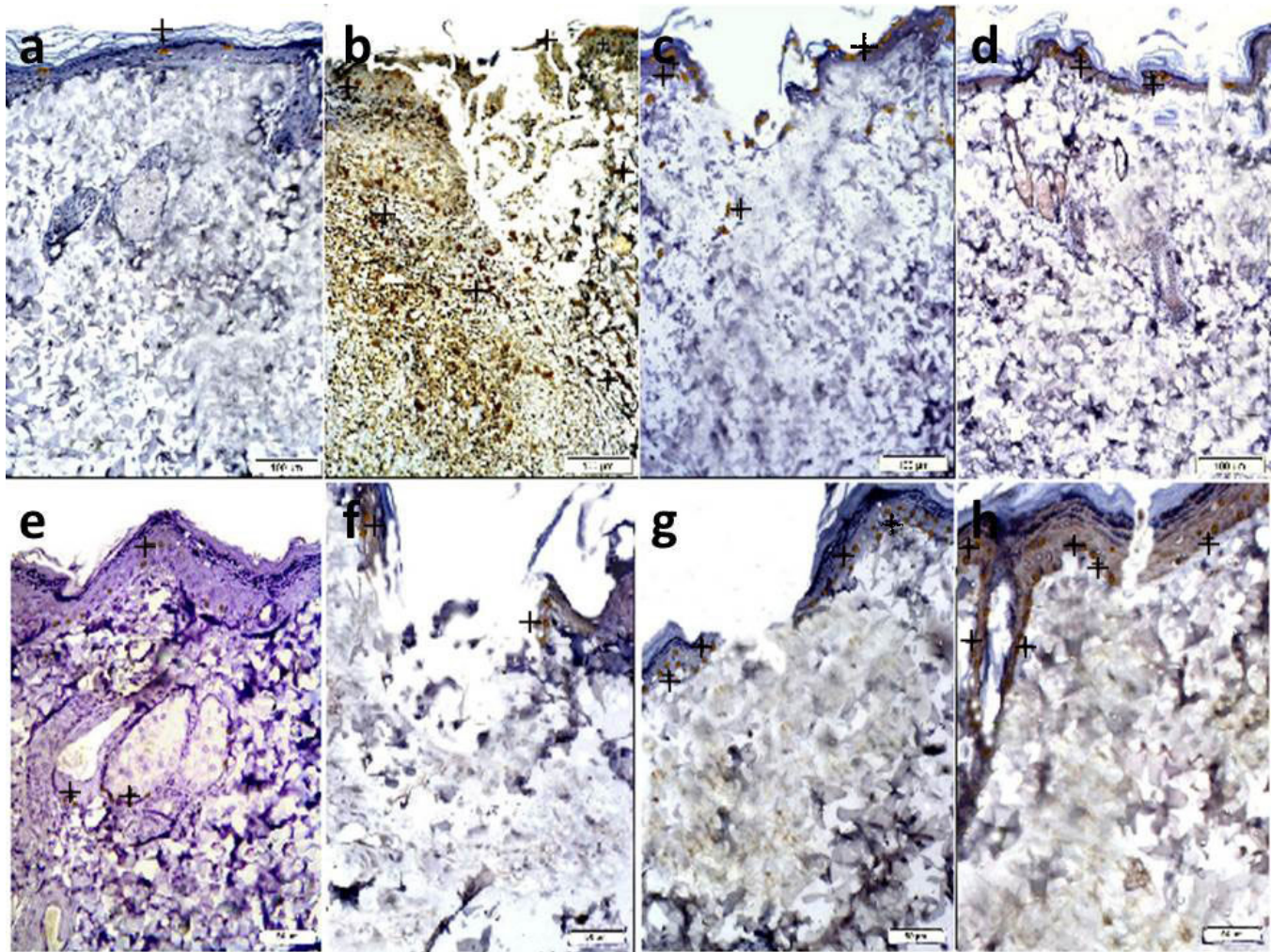


**Fig. 6** showing +ve IE (+) in: (a) few surface keratinocytes in 1st group I. (b) multiple keratinocytes and dermal cells in 2nd group. (c) some keratinocytes and dermal cells in 3rd group. (d) few keratinocytes and dermal cells in 4th group (Caspase3 immunostaining, x100). (e) some PCNA +ve nuclei in epidermis and in lining of a follicle and sebaceous glands in 1st group. (f) few PCNA +ve nuclei in epidermis in 2nd group. (g) multiple PCNA +ve nuclei in epidermis in 3rd group. (h) multiple PCNA +ve nuclei in epidermis and in lining of a follicle in 4th group (PCNA immunostaining, x200).



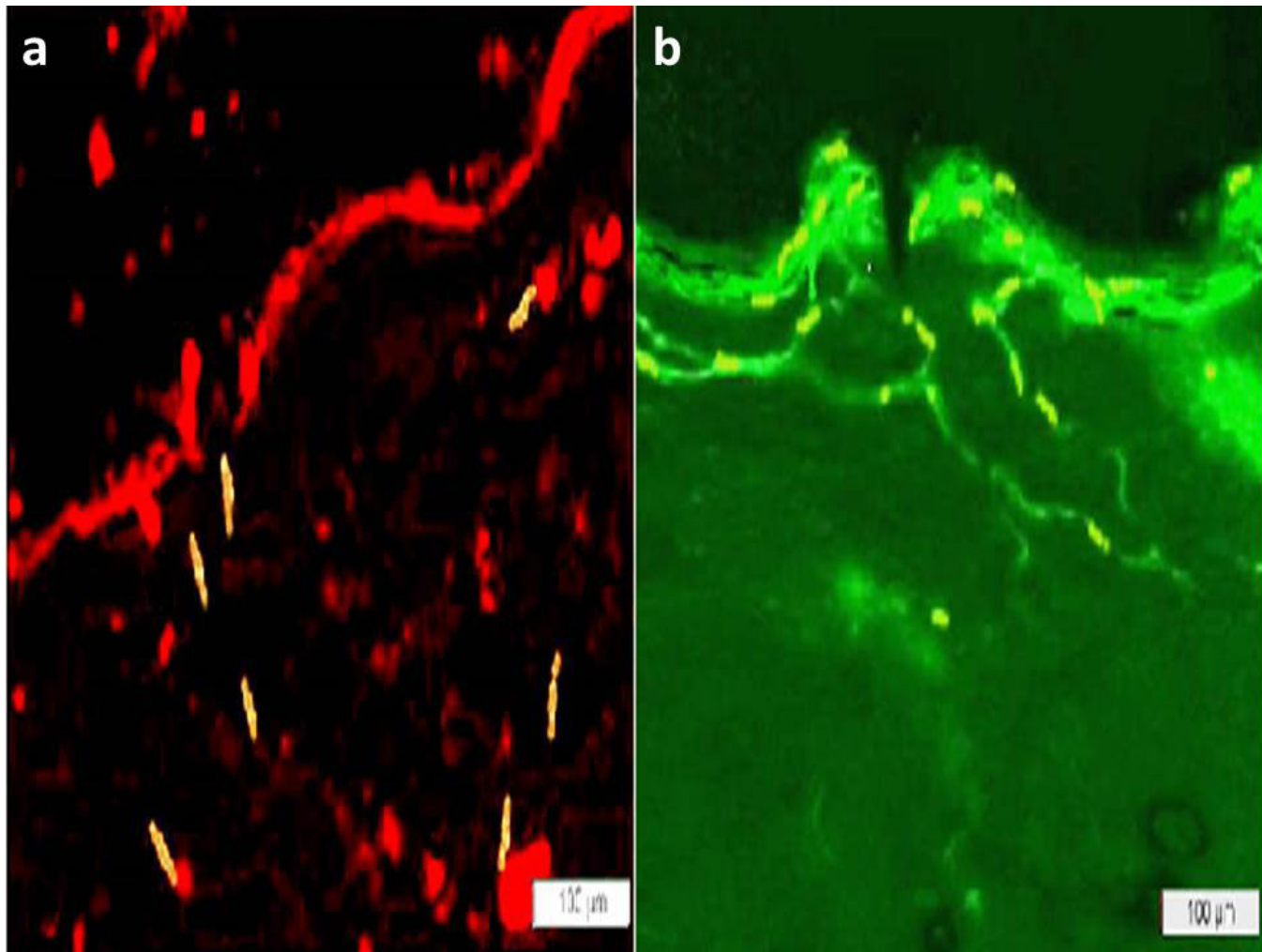


Fig. 7 showing: (a) multiple PKH26 tagged cells in 3rd group (PKH26, x 100). (d) multiple GFP tagged cells in 4th group (GFP, x 100).

**Table 1:** Wound surface area (Mean  $\pm$  SD) at the end of 1<sup>st</sup> and 3<sup>rd</sup> weeks in different groups

Groups	1 <sup>st</sup> week	3 <sup>rd</sup> week
2 <sup>nd</sup> Group	372842.73 $\pm$ 54485.501	395602.2 $\pm$ 59779.60
3 <sup>rd</sup> Group	130703.0 $\pm$ 13740.84*	90382.6 $\pm$ 14516.15*
4 <sup>th</sup> Group	4759.6 $\pm$ 747.10 <sup>^</sup>	3802.8 $\pm$ 727.42 <sup>^^</sup>

\*significant compared to 2<sup>nd</sup> group at end of 1<sup>st</sup> and 3<sup>rd</sup> weeks

<sup>^</sup>significant compared to 3<sup>rd</sup> group at end of 1<sup>st</sup> and 3<sup>rd</sup> weeks

**Table 2:** Mean  $\pm$  SD of the distance of epidermal margins, area % of pale stained collagen fibers, area% of CK3 +ve IE, area % of caspase3 +ve IE, area% of PCNA +ve nuclei and PCR values of SERCA2 gene in control and experimental groups

Groups	Distance of epidermal margins	Area% of pale stained collagen fibers	Area% of CK3 +ve IE	Area% of caspase3 +ve IE	Area% of PCNA +ve nuclei	PCR
1 <sup>st</sup> Group	0	0	27.87 $\pm$ 2.34	0.46 $\pm$ 0.03	12.89 $\pm$ 0.18e	1.45 $\pm$ 0.25
2 <sup>nd</sup> Group	59.98 $\pm$ 5.31	76.71 $\pm$ 11.29	6.65 $\pm$ 12.11c	19.21 $\pm$ 1.29c	4.18 $\pm$ 0.43	0.19 $\pm$ 0.03c
3 <sup>rd</sup> Group	28.99 $\pm$ 3.32a	35.04 $\pm$ 6.89a	13.46 $\pm$ 3.08d	5.22 $\pm$ 1.05d	20.05 $\pm$ 3.21f	0.46 $\pm$ 0.07d
4 <sup>th</sup> Group	12.98 $\pm$ 2.31b	5.94 $\pm$ 1.19b	21.32 $\pm$ 5.23	0.61 $\pm$ 0.04	31.98 $\pm$ 2.97c	1.28 $\pm$ 0.14

<sup>a</sup>significant compared to 2<sup>nd</sup> group II.

<sup>b</sup>significant compared to 2<sup>nd</sup> group and 3<sup>rd</sup> group.

<sup>c</sup>significant compared to other groups.

<sup>d</sup>significant compared to 1<sup>st</sup> group and 4<sup>th</sup> group.

<sup>e</sup>significant compared to 2<sup>nd</sup> group.

<sup>f</sup>significant compared to 1<sup>st</sup> group and 2<sup>nd</sup> group.

## DISCUSSION

Diabetic wounds present a major management problem since they heal slowly, are challenging to control and may persist for weeks. Therefore, the objective of clinical treatment would be to attempt to rapidly close the skin lesions with perfect functioning results<sup>[29]</sup>. The current study compared the therapeutic effect of SERCA2 gene modified AdMSCs to non-transfected AdMSCs on induced wound in male albino rat model of T1DM.

The current work proved that stem cell therapy had an ameliorating impact on diabetic wound damage generated in the rat model. Measurements of wound surface area, phenotypic, qualitative and quantitative evaluations were confirmative.

The wound surface area can be considered a landmark between a complicated wound and a wound having high healing potential. The measurement also is crucial to assess effectiveness of treatment regimens<sup>[30]</sup>

The mean serum glucose levels in 2<sup>nd</sup> group were found to denote significant increase versus 1<sup>st</sup>, 3<sup>rd</sup> and 4<sup>th</sup> groups. In accordance, hyperglycemia represents a major factor in elevated protein glycosylation. In addition, production of free radicals try to glucose oxidation that encourage cell membrane lipid peroxidation, consequently attenuating the membrane<sup>[31]</sup>.

Second group demonstrated wide separation of the wound edges, detached parts of the epidermis, disrupted dermal fibers, detached sebaceous glands. Follicles lined by one layer of cells, multiple microfollicles, epidermal vacuoles, loss of the granules in the granular cell layer, multiple atypical and multiple pale fibers were observed in the dermis. Recently, Lin et al,<sup>[32]</sup> noticed hypoxia, reduced hemoglobin and tissue blood volume besides inflammatory criteria in diabetic wound that lead to delayed healing.

In 2<sup>nd</sup> group, localized dense +ve CK3 IE was found and less dense IE was observed in other areas of thin epidermis and in hair follicles with reduced lining at the wound. Loss of CK3 IE was demonstrated in multiple areas of the epidermis and dense +ve IE was seen at the horny layer in some other areas of the intact skin. A significant decrease was evidenced versus control and treated groups. Concomitantly, Sharma et al<sup>[33]</sup> documented delayed healing, epithelialization and keratinization in diabetic wounds as a consequence of excessive protease activity.

In 2<sup>nd</sup> group caspase3 IE was found in many keratinocytes and dermal cells, that was confirmed morphometrically in the diabetic rats versus all other groups. As confirmed by Liu et al<sup>[34]</sup>, who stated that oxidant-nonoxidant imbalance induces apoptosis-related genes expression, stimulating cell death via caspase-3 signaling pathways. In addition, few PCNA +ve nuclei were detected in the epidermis. In accordance, it was proved that the accumulated reactive oxygen species could lead to delayed healing try to cytoplasmic, nucleic acids damage and lipid peroxidation<sup>[35]</sup>.

The mean Ca ion concentration, mean SERCA2 protein and mean SERCA2 gene levels recorded a significant decrease in 2<sup>nd</sup> group versus other groups and in 3<sup>rd</sup> group versus 1<sup>st</sup> and 4<sup>th</sup> groups, which can be related to lack of SERCA2 transfection in 3<sup>rd</sup> group. Concomitantly, Wu et al<sup>[36]</sup> reported a dysfunctional epithelial barrier in diabetic rats that was correlated to Ca<sup>2+</sup> disturbance and could be referred to mis-handled sarcoplasmic reticulum Ca<sup>2+</sup>-ATPase2 (SERCA2). Ferroni et al<sup>[37]</sup> added that the expression of genes related to recycling and stem cell potency were downregulated in diabetes.

Third group (AdMSCs treated diabetic group) revealed less widely separated edges of the wound confirmed morphometrically by distance between edges versus diabetic group. Micro follicles, follicles lined by multiple layers of cells and sebaceous glands were seen. Focal loss of granules, few vacuolated keratinocytes and multiple pale dermal fibers, confirmed morphometrically by area% versus diabetic group, were observed. The previously mentioned changes denoted amelioration of inflammatory and degenerative morphological features, consequently, favourable healing and regeneration.

Accordingly, Hilton et al<sup>[38]</sup> proved that MSCs can biomechanically affect wound closure as MSCs induced higher and more complete collagen contraction versus dermal fibroblasts. They also participate in the regulation of inflammation, and inter-cellular communications in the local tissues concerning wound repair.

In 3<sup>rd</sup> group, dense +ve CK3 IE at the horny layer, less dense IE in some areas of the epidermis and in the lining of the follicles were noticed at the wound. In addition, less dense +ve IE was detected in multiple areas besides loss of IE in localized areas of the epidermis and in the lining of few follicles. The previous results were confirmed morphometrically by the mean area% versus diabetic group. In agreement, Kanji et al,<sup>[39]</sup> recorded improved re-epithelialization, keratinization and neovascularization of cutaneous wounds in diabetic mice by hemopoietic SCs therapy.

Less obvious caspase3 IE was found on the contrary in 3<sup>rd</sup> group which was expressed as significant decrease morphometrically versus 2<sup>nd</sup> group. In addition, multiple PCNA +ve epidermal nuclei were proved by a significant increase in mean count 1<sup>st</sup> and 2<sup>nd</sup> versus groups. Concomitantly, Zafari et al<sup>[40]</sup> stated that diabetic wound healing responded to stem cells' therapy via growth factor stimulation and down-regulation of apoptosis genes, in addition to their promising proliferative, migratory, clonogenic and immunomodulatory properties.

In 3<sup>rd</sup> and 4<sup>th</sup> groups, many PKH26 tagged and many GFP tagged cells were visualized at and around wound site. These findings confirmed migration of cultured non-transfected and gene modified AdMSCs cells to wound area, concluding enhancement of repair.

Fourth group revealed minimal separation of wound edges, normal appearance of epidermis, multiple micro follicles, multiple sebaceous glands and fully developed hair follicles. Normal appearance of granular layer and reduced thickness of the wound edge were detected. In addition, few pale fibers were evident among the normal collagen fibers in the dermis. A significant decrease of distance between wound edges and area% of pale was confirmative in 4<sup>th</sup> group compared to the other groups. This can be referred to higher efficiency of regenerative plasticity of SERCA2 modified AdMSCs and transdifferentiation into epidermal cells and appendages. In support, da Silva Vasconcelos *et al*<sup>[41]</sup> found that higher SERCA expression and cytosolic Ca<sup>2+</sup> level are accompanied by improving structural and functional tissue capacity in diabetic animals.

In the 4<sup>th</sup> group, dense +ve CK3 IE was demonstrated in some areas, less dense IE in multiple epidermal areas and follicles at the wound. In addition localized loss of IE was noticed. Focal loss of IE was accidentally found in the rest of epidermis and in follicles, denoting reinforcement of cytoskeletal element. This finding was proved morphometrically versus diabetic and AdMSCs treated diabetic groups. Going with, massive cytoskeletal rearrangement was concluded by Kovuru *et al*<sup>[42]</sup> by active SERCA pumps that accumulates Ca<sup>2+</sup> against its electrochemical gradient in the ER and the capacity of this Ca<sup>2+</sup> store is increased by the presence of Ca<sup>2+</sup> binding proteins in the lumen of the reticulum.

Concerning caspase3 IE in 4<sup>th</sup> group, few keratinocytes and dermal cells showed +ve IE and a significant decrease was reported versus 2<sup>nd</sup> and 3<sup>rd</sup> groups. In addition, multiple PCNA+ve epidermal nuclei were evident and in lining of follicles, denoting a statistically significant versus all groups. These results confirmed very minimal residual degenerative changes. Concomitantly, Britzolaki *et al*<sup>[43]</sup> confirmed that for cells and tissues to properly regenerate, repair, and function, intracellular Ca<sup>2+</sup> homeostasis is a vital regulator. Neuropathological disorders have been linked to SERCA-mediated calcium dyshomeostasis, pointing to SERCA gene as potential innovative treatment for these and other diseases.

## CONCLUSION

It can be concluded that SERCA2 gene modified AdMSCs therapy induced sterile, fast and complete wound healing more noticeable than that induced by AdMSCs therapy. The measurement of wound surface area, phenotypic and quantitative studies proved this therapeutic effect.

## CONFLICT OF INTERESTS

There are no conflicts of interest.

## REFERENCES

1. Zheng Y, Zheng S, Fan X, Li L, Xiao Y, Luo P, Liu Y, Wang L, Cui Z, He F, Liu Y, Xiao S, Xia Z. Amniotic Epithelial Cells Accelerate Diabetic Wound Healing by Modulating Inflammation and Promoting Neovascularization. *Stem Cells Int.* 2018; 2018:1082076-1082085. DOI:10.1155/2018/1082076.
2. Li M, Yu H, Pan H, Zhou X, Ruan Q, Kong D, Chu Z, Li H, Huang J, Huang X, Chau A, Xie W, Ding Y, Yao P. Nrf2 Suppression Delays Diabetic Wound Healing Through Sustained Oxidative Stress and Inflammation. *Front Pharmacol.* 2019; 10:1099-1110. DOI: 10.3389/fphar.2019.01099.
3. Hu MS, Borrelli MR, Lorenz HP, Longaker MT, Wan DC. Mesenchymal Stromal Cells and Cutaneous Wound Healing: A Comprehensive Review of the Background, Role, and Therapeutic Potential. *Stem Cells Int.* 2018; 2018:6901983 -6901995. DOI: 10.1155/2018/6901983.
4. Rothrauff BB, Jorge A, de Sa D, Kay J, Fu FH, Musahl V. Anatomic ACL reconstruction reduces risk of post-traumatic osteoarthritis: a systematic review with minimum 10-year follow-up. *Knee Surg Sports Traumatol Arthrosc.* 2020; 28(4):1072-1084. DOI: 10.1007/s00167-019-05665-2.
5. Zorn-Kruppa M, Volksdorf T, Ueck C, Zöller E, Reinshagen K, Ridderbusch I, Bruning G, Houdek P, Moll I, Brandner JM. Major cell biological parameters of keratinocytes are predetermined by culture medium and donor source. *Exp Dermatol.* 2016; 25(3):242-244. DOI: 10.1111/exd.12922.
6. Ahmad I, Muneer KM, Chang ME, Nasr HM, Clay JM, Huang CC, Yusuf N. Ultraviolet Radiation-Induced Downregulation of SERCA2 Mediates Activation of NLRP3 Inflammasome in Basal Cell Carcinoma. *Photochem Photobiol.* 2017; 93(4):1025-1033. DOI: 10.1111/php.12725
7. Lee SE, Lee SH. Skin Barrier and Calcium. *Ann Dermatol.* 2018; 30(3):265-275. DOI: 10.5021/ad.2018.30.3.265
8. Yu X, Liang X, Xie H, Kumar S, Ravinder N, Potter J, de Mollerat du Jeu X, Chesnut JD. Improved delivery of Cas9 protein/gRNA complexes using lipofectamine CRISPRMAX. *Biotechnol Lett.* 2016; 38(6):919-929. DOI: 10.1007/s10529-016-2064-9
9. Hidaka R, Machida M, Fujimaki S, Terashima K, Asashima M, Kuwabara T. Monitoring neurodegeneration in diabetes using adult neural stem cells derived from the olfactory bulb. *Stem Cell Res Ther.* 2013; 4(3):51-61. DOI: 10.1186/scrt201.
10. Bhansali S, Kumar V, Saikia UN, Medhi B, Jha V, Bhansali A, Dutta P. Effect of mesenchymal stem cells transplantation on glycaemic profile and their localization in streptozotocin induced diabetic Wistar rats. *Indian J Med Res.* 2015; 142(1):63-71. DOI: 10.4103/0971-5916.162116.
11. Lee YS, Kwon ST, Kim JO, Choi ES. Serial MR imaging of intramuscular hematoma: experimental study in a rat model with the pathologic correlation. *Korean J Radiol.* 2011; 12(1):66-77. DOI: 10.3348/kjr.2011.12.1.66.



12. Bassiony HS, Zickri MB, Metwally HG, Elsherif HA, Alghandour SM, Sakr W. Comparative Histological Study on the Therapeutic Effect of Green Tea and Stem Cells in Alzheimer's Disease Complicating Experimentally Induced Diabetes. *Int J Stem Cells*. 2015; 8(2):181-190. DOI: 10.15283/ijsc.2015.8.2.181.
13. Espina M, Jülke H, Brehm W, Ribitsch I, Winter K, Delling U. Evaluation of transport conditions for autologous bone marrow-derived mesenchymal stromal cells for therapeutic application in horses. *PeerJ*. 2016; 4:e1773-1795. DOI: 10.7717/peerj.1773.
14. Li H, Fu X, Ouyang Y, Cai C, Wand J, Sun T. Adult bone marrow-derived mesenchymal stem cells contribute to wound healing of skin appendages. *Cell and Tissue Research* 2006; 326(3):725-736. DOI: 10.1007/s00441-006-0270-9.
15. Aboul-Fotouh GI, Zickri MB, Metwally HG, Ibrahim IR, Kamar SSI. Comparative Study on the Therapeutic Effect of Atorvastatin and Stem Cells on Amiodarone Induced Lung Injury in Male Rat. *Int J Stem Cells*. 2016; 8(2):170-180. DOI: 10.15283/ijsc.2015.8.2.170.
16. Ude CC, Shamsul BS, Ng MH, Chen HC, Norhamdan MY, Aminuddin BS, Ruszymah BH. Bone marrow and adipose stem cells can be tracked with PKH26 until post staining passage 6 in in vitro and in vivo. *Tissue Cell*. 2012; 44:156-163. DOI: 10.1016/j.tice.2012.02.001.
17. Tupling AR, Bombardier E, Gupta SC, Hussain D, Vigna C, Bloemberg D, Quadrilatero J, Trivieri MG, Babu GJ, Backx PH, Periasamy M, MacLennan DH, Gramolini AO. Enhanced Ca<sup>2+</sup> transport and muscle relaxation in skeletal muscle from sarcolipin-null mice. *Am J Physiol Cell Physiol*. 2011; 301(4):841-858. DOI: 10.1152/ajpcell.00409.2010.
18. Mars T, Strazisar M, Mis K, Kotnik N, Pegan K, Lojk J, Grubic Z, Pavlin M. Electrotransfection and lipofection show comparable efficiency for in vitro gene delivery of primary human myoblasts. *J Membr Biol*. 2015; 248(2):273-283. DOI: 10.1007/s00232-014-9766-5.
19. Gruber SJ, Cornea RL, Li J, Peterson KC, Schaaf TM, Gillispie GD, Dahl R, Zsebo KM, Robia SL, Thomas DD. Discovery of enzyme modulators via high-throughput time-resolved FRET in living cells. *J Biomol Screen*. 2014; 19(2):215-222. DOI: 10.1177/1087057113510740.
20. Foltynski P, Ciechanowska A, Ladyzynski P. Wound surface area measurement methods. *Biocybernetics and Biomedical Engineering*. 2021;(41):1454-1465. <https://doi.org/10.1016/j.bbe.2021.04.011>.
21. Iranpour FG, Kheiri S. Coadministration of calcium chloride with lead acetate can improve motility of cauda epididymal spermatozoa in Swiss white mice. *Int J Reprod BioMed*. 2016; 14(2):141-144. PMID: 27200429. PMID: PMC4869154.
22. Aziz MT, El-Asmar MF, Rezaq AM, Wassef MA, Fouad H, Roshdy NK, Ahmed HH, Rashed LA, Sabry D, Taha FM, Hassouna A. Effects of a novel curcumin derivative on insulin synthesis and secretion in streptozotocin-treated rat pancreatic islets in vitro. *Chin Med*. 2014; 9(1):3-14. DOI: 10.1186/1749-8546-9-3.
23. Trost SU, Belke DD, Bluhm WF, Meyer M, Swanson E, Dillmann WH. Overexpression of the sarcoplasmic reticulum Ca<sup>2+</sup>-ATPase improves myocardial contractility in diabetic cardiomyopathy. *Diabetes*. 2002; 51(4):1166-1171. DOI: 10.2337/diabetes.51.4.1166.
24. Kiernan J K. Histological and Histochemical methods. In: *Theory and practice*. 3<sup>rd</sup> edition, Arnold Publisher, London, New York, and New Delhy; 2001:111-162.
25. Bancroft JD, Gamble M. Connective tissue stains. In: *Theory and Practice of Histological Techniques*, sixth edition. Elsevier Health Sciences, Churchill Livingstone, Edinburgh, London, Oxford, New York, Philadelphia, St Louis, Sydney and Toronto; 2008:150. <https://doi.org/10.1097/NEN.0b013e31817e2933>.
26. Suvarna SK, Layton C, Bancroft JD: *Bancroft's Theory and Practice of Histological Techniques*. 7th ed., New York, USA: Elsevier Health Sciences, Churchill Livingstone; (2012) pp. 215–239.
27. Pu T, Guo P, Qiu Y, Chen S, Yang L, Sun L, Ye F, Bu H. Quantitative real-time polymerase chain reaction is an alternative method for the detection of HER-2 amplification in formalin-fixed paraffin-embedded breast cancer samples. *Int J Clin Exp Pathol*. 2015; 8(9):10565-10574. PMID: 26617766. PMID: PMC4637581
28. Emsley R, Dunn G, White I. Mediation and moderation of treatment effects in randomized controlled trials of complex interventions. *Stat Methods Med Res*. 2010; 19(3):237-270. DOI: 10.1177/0962280209105014.
29. Kim JE, Lee JH, Kim SH, Jung Y. Skin Regeneration with Self-Assembled Peptide Hydrogels Conjugated with Substance P in a Diabetic Rat Model. *Tissue Eng Part A*. 2018; 24(1-2):21-33. DOI: 10.1089/ten.TEA.2016.0517.
30. Mehl AA, Schneider Jr B, Schneider FK, Carvalho BHK. Measurement of wound area for early analysis of the scar predictive factor. *Rev. Latino-Am.Enfermagem*. 2020;28: e3299-3307. DOI: 10.1590/1518-8345.3708.3299.
31. Arise RO, Akapa TC, Adigun MA, Yekeen AA, Oguntibeju OO. Normoglycaemic, normolipidaemic and antioxidant Effects of ethanolic extract of *Acacia ataxacantha* root in streptozotocin - induced Diabetic Rats. *Notulae Botanicae Horti Agrobotanici Cluj- napoca*. 2016; 8:144-150. DOI:10.15835/nsb.8.2.97570.

32. Lin BS, Chang CC, Tseng YH, Li JR, Peng YS, Huang YK. Using Wireless Near-Infrared Spectroscopy to Predict Wound Prognosis in Diabetic Foot Ulcers. *Adv Skin Wound Care*. 2020; 33(1):1-12. DOI: 10.1097/01.ASW.0000613552.50065.d5.
33. Sharma S, Schaper N, Rayman G. Microangiopathy: Is it relevant to wound healing in diabetic foot disease? *Diabetes Metab Res Rev*. 2020; 36 Suppl 1:e3244. DOI: 10.1002/dmrr.3244.
34. Liu Q, Si T, Xu X, Liang F, Wang L, Pan S. Electromagnetic radiation at 900 MHz induces sperm apoptosis through bcl-2, bax and caspase-3 signaling pathways in rats. *Reprod Health*. 2015; 12:65. doi: 10.1186/s12978-015-0062-3.
35. Oso BJ, Abey N, Oyeleke MO, Olowookere B. Comparative study of the in vitro antioxidant properties of methanolic extracts of *Chromolaena odorata* and *Ageratum conyzoides* use in wound healings. *Int Ann Sci*, 2019; 6(1): 8-12. DOI:10.21467/ias.6.1.8-12.
36. Wu Q, Lei X, Chen L, Zheng Y, Huang H, Qian C, Liang Z. Autologous platelet-rich gel combined with in vitro amplification of bone marrow mesenchymal stem cell transplantation to treat the diabetic foot ulcer: a case report. *Ann Transl Med*. 2018; 6(15):307. DOI: 10.21037/atm.2018.07.12.
37. Ferroni L, Gardin C, Dalla Paola L, Campo G, Cimaglia P, Bellin G, Pinton P, Zavan B. Characterization of Dermal Stem Cells of Diabetic Patients. *Cells*. 2019; 8(7):729. DOI: 10.3390/cells8070729.
38. Hilton SA, Dewberry LC, Hodges MM, Hu J, Xu J, Liechty KW, Zgheib C. Mesenchymal stromal cells contract collagen more efficiently than dermal fibroblasts: Implications for cytotherapy. *PLoS One*. 2019; 14(7):e0218536. DOI: 10.1371/journal.pone.0218536.
39. Kanji S, Das M, Joseph M, Aggarwal R, Sharma SM, Ostrowski M, Pompili VJ, Mao HQ, Das H. Nanofiber-expanded human CD34+ cells heal cutaneous wounds in streptozotocin-induced diabetic mice. *Sci Rep*. 2019; 9(1):8415. DOI: 10.1038/s41598-019-44932-7.
40. Zafari F, Shirian S, Sadeghi M, Teimourian S, Bakhtiyari M. CD93 hematopoietic stem cells improve diabetic wound healing by VEGF activation and downregulation of DAPK-1. *J Cell Physiol*. 2020; 235(3):2366-2376. DOI: 10.1002/jcp.29142.
41. da Silva Vasconcelos E, Kalinin AL, Cipriano RC, Dos Santos Beserra S, Lopes AG, da Costa Leite CA, Monteiro DA. Effects of feeding and digestion on myocardial contractility and expression of calcium-handling proteins in Burmese pythons (*Python molurus*). *Comp Biochem Physiol B Biochem Mol Biol*. 2020; 240:110371. DOI: 10.1016/j.cbpb.2019.110371.
42. Kovuru N, Raghuvanshi S, Sharma DS, Dahariya S, Palapati A, Gutti RK. Endoplasmic reticulum stress induced apoptosis and caspase activation is mediated through mitochondria during megakaryocyte differentiation. *Mitochondrion*. 2020; 50:115-120. DOI: 10.1016/j.mito.2019.10.009.
43. Britzolaki A, Saurine J, Klocke B, Pitychoutis PM. A Role for SERCA Pumps in the Neurobiology of Neuropsychiatric and Neurodegenerative Disorders. *Adv Exp Med Biol*. 2020; 1131:131-161. DOI: 10.1007/978-3-030-12457-1\_6.

## الملخص العربي

## تأثير الخلايا الجذعية المنقولة بجين السيركا ٢ مقارنة بالخلايا الجذعية على الجرح المستحث في مرض السكري من النوع الأول لنموذج الجرذ الأبيض الذكر

مها بليغ زكري<sup>١،٢</sup>، هالة أحمد الشريف<sup>١</sup>، زينب محمد الطيب<sup>٣</sup>، أحلام محمد غريب<sup>٣</sup>، أمل مولود الشيباني<sup>٤</sup>، راضية مصباح أحمد<sup>٥</sup>، أماني السيد حمود<sup>٥</sup>

<sup>١</sup> قسم الأنسجة الطبية، كلية الطب، جامعة القاهرة، مصر  
<sup>٢</sup> كلية طب الفم والأسنان، جامعة المستقبل، مصر FUE  
<sup>٣</sup> قسم الأنسجة الطبية، كلية الطب، جامعة حلوان، مصر  
<sup>٤</sup> قسم الأحياء، كلية الطب، جامعة الزاوية، ليبيا  
<sup>٥</sup> قسم التشريح والأجنة، كلية الطب، جامعة القاهرة، مصر

**الخلفية والأهداف:** من الصعب إدارة جروح مرضى السكري. بالنسبة لتكاثر الخلايا والهجرة والتمايز والتجديد، يعد التوازن داخل الخلايا  $+Ca^{2+}$  أمرًا بالغ الأهمية. تبين أن الشبكة الساركوبلازمية  $+Ca^{2+}$  ATPase<sup>٢</sup> (SERCA<sup>٢</sup>) تتحكم في مستوى  $+Ca^{2+}$  في الخلايا الكيراتينية. تعتبر الخلايا الجذعية الوسيطة المشتقة من الدهون (AdMSCs) ضرورية لإصلاح الجروح. تمت دراسة التأثير العلاجي لـ AdMSCs المعدلة جينيًا SERCA<sup>٢</sup> ومقارنتها مع تأثير AdMSCs تجريبيًا جرح السكري من النوع ١.

**الطرق والنتائج:** تم تصنيف ٤٢ فأرًا ذكرًا إلى: مجموعة التبرع: تم استخدام ثلاثة منها لزراعة الخلايا الجذعية والتنميط الظاهري ووضع العلامات وتحضير SERCA<sup>٢</sup>. المجموعة الأولى I (المجموعة الضابطة): تسعة فئران، المجموعة الثانية (المجموعة الجريحة): تم حقن عشرة فئران بالستربتوزوتوسين (STZ) داخل الصفاق (IP) ٥٠ ملغ، ثم تم تعريض الفئران لتحرير الجرح (شق الجلد ١ × ١ سم). المجموعة الثالثة (علاج AdMSCs): عشرة فئران، تم حقن IP بـ AdMSCs ١ × ١٠<sup>٦</sup>. المجموعة الرابعة (مجموعة AdMSCs المعدلة بواسطة SERCA<sup>٢</sup>): عشرة فئران، تم حقن IP باستخدام AdMSCs المعدل ١ × ١٠<sup>٦</sup> بواسطة SERCA<sup>٢</sup>. وبحلول نهاية الأسبوعين الأول والثالث، تم قياس مساحة سطح الجرح الناجم عن مرض السكري. تم خدش المجموعتين الأولى والثانية والثالثة والرابعة بعد ثلاثة أسابيع من تشخيص مرض السكري. تم إجراء الدراسات الهستولوجية والكيميائية الحيوية والمظهرية والكمية. في المجموعة الثانية، شوهدت تغيرات التهابية وتليفية وتنكسية في منطقة الجرح وفي الجلد السليم. في المجموعتين الثالثة والرابعة تم تحسين هذه التغييرات، ولاحظت أكثر في المجموعة الرابعة. وفي المجموعة الثانية، وجد فرق كبير في مساحة سطح الجرح. تم تأكيد التغييرات المظهرية والكمية عن طريق نسبة الجلوكوز في الدم وتركيز الجلد  $+Ca^{2+}$  وتحليل الكيمياء.